Recent Developments in the HUGIN AUV Terrain Navigation System

Kjetil Bergh Ånonsen and Ove Kent Hagen
Norwegian Defence Research Establishment (FFI)
Kjeller, Norway
Email: kjetil-bergh.anonsen@ffi.no

***Abstract*— This paper describes recent developments in the HUGIN AUV terrain navigation system, which uses terrain measurements in order to provide submerged position updates for the main inertial navigation system. In previous versions of the system, a prior bathymetric map database has been required, sometimes restricting the use of the system. To relax this requirement, a real-time map generator has been implemented, such that the vehicle is able to build its own map during the mission. When returning to the mapped area, the system can use this map in order to obtain a terrain navigation fix, thus reducing the uncertainty of the navigation system. Results from a sea trial of the concept are presented, in which the system effectively brings the navigation uncertainty down from more than 50 to about 10 meters. Further results, using the system in the traditional manner with a prior map database, are also included.**

I. Introduction

Precise underwater navigation is crucial in a number of marine applications. This paper focuses on navigation of autonomous underwater vehicles (AUVs), although the techniques described can also be used by other types of underwater vehicles, like submarines and remotely operated vehicles (ROVs).

Most AUV navigation systems are based on inertial navigation, see e.g. [1]. Inertial navigation systems drift off with time, even when velocity aiding is used. In order to allow extensive submerged operations, additional position fixes are needed. As GPS is not available underwater, one is often dependent on acoustic aiding of the vehicle, either from a mother ship or by using underwater acoustic transponders. In order to increase the autonomy of the vehicle and avoid costly pre-deployment of underwater transponders, terrain-based navigation is a favorable alternative. As an AUV in many cases carries a bathymetric sensor, it is natural to utilize bathymetric information in the navigation of the vehicle. For the methods discussed here it is assumed that a bathymetric map database of the area exists, but this can be created by the system's real-time map generator if necessary. Any sensor that is able to measure the altitude of the vehicle can be used for terrain navigation, and the effectiveness of the sensor for this purpose is determined by the swath width of the sensor. A sensor with multiple measurements in each ping, covering a large swath, like a multibeam echo sounder (MBE), leads to faster convergence of the terrain navigation algorithms than a single measurement sensor, like an acoustic altimeter. In the test presented in this paper, an EM 2000 MBE was used as terrain measuring sensor, providing up to 111 measurements from each ping.

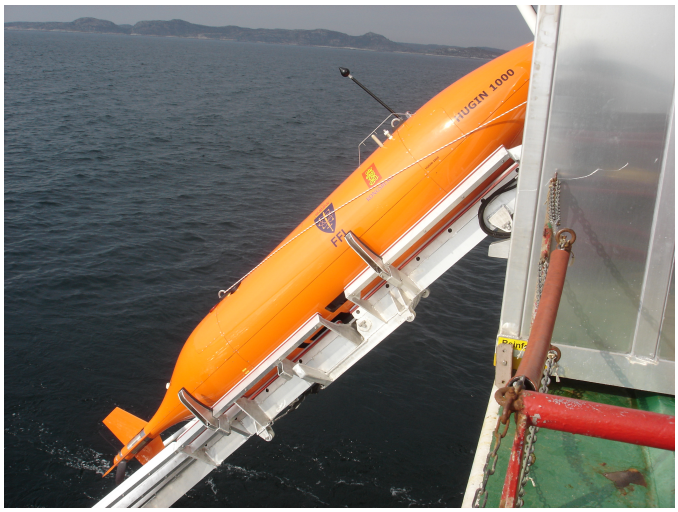

Fig. 1. The HUGIN 1000 HUS seconds before launch from FFI's research vessel H.U. Sverdrup II.

Terrain-based navigation has been used for decades in aircraft and cruise missiles [2], [3]. For underwater applications some work has been published over the last decade [4], [5], [6]. A variety of different terrain-based navigation methods have been proposed in the literature. Among the more sophisticated are the Bayesian methods, in which the position of the vehicle is estimated using a state-space model. Due to the strong nonlinearity of the measurements, Kalman filter-based methods have proven not to be suitable in most cases. Instead nonlinear Bayesian methods like point mass (PMF) and particle filters (PF) have been successfully applied to underwater navigation [3], [5].

Terrain aided navigation for the HUGIN AUV family has been a research topic at FFI for several years, [5]–[8]. This research has led to the development of a real-time terrain navigation system for the HUGIN vehicles, named TerrP. The TerrP system is used as an external position aiding method for the main inertial navigation system (NavP). The TerrP system is thoroughly described in [9]. The HUGIN aided inertial navigation system is described in [1]. Alternative real-time underwater terrain navigation systems were described in [10],

[11].

This paper focuses on recent developments in the HUGIN terrain navigation system. The most prominent new feature is a real-time map generator, which can be used to build a map from the in-mission bathymetric measurements. Later, when returning to the mapped area, terrain navigation methods can be used in order to obtain position fixes relative to this map, thus reducing the navigation uncertainty to the uncertainty present at the time of the mapping. This technique will be referred to as '*in situ* sequential mapping and localization' and boarders the vast research area of simultaneous localization and mapping (SLAM) [12], [13], but as the mapping and localization phases are carried out sequentially, it is not SLAM in the strict sense.

The outline of the paper is as follows. In Section II a brief mathematical description of the terrain navigation algorithms are given, before a short description of the HUGIN terrain navigation system follows in Section III. In Section IV results from a recent sea trial of the system are presented, before conclusions and suggestions for future work are given in Section V.

II. Terrain Navigation Algorithms

In our application, the measurements represent the total water depth at the MBE footprint, i.e. the sum of the AUV depth, calculated from pressure sensor measurements, and the altitude measurements from the MBE. To be able to compare these measurements to the depth values in the map data base, they must be converted to the same vertical datum as the map database, usually mean sea level.

In [6], it was shown how errors in the pressure-to depth conversion and tide effect compensation can lead to inaccuracies and errors in the terrain navigation position estimates, and how this problem can be solved by including estimation of the depth bias in the algorithms. In the tests described in this paper, a 2-dimensional estimation model was used. Depth bias issues may however be countered using relative depth profiles, i.e. extracting the mean value from the measured profiles as well as from the map profile.

A. System Model

We consider the following model for the motion of our AUV,

$$\mathbf{x}_{k+1} = \mathbf{x}_k + \mathbf{u}_k + \mathbf{v}'_k + \mathbf{v}_k, \tag{1}$$

$$\mathbf{v}'_{k+1} = \mathbf{g}(\mathbf{v}'_k) + \mathbf{v}''_k, \tag{2}$$

where $\mathbf{x}_k = (x_N, x_E)^T$ is the AUV position vector, $\mathbf{u}_k$ is the position change calculated from the inertial navigation system, and $\mathbf{v}_k$ and $\mathbf{v}''_k$ are independent white noise sequences. Equation (2) models the strongly correlated error propagation of the inertial navigation system. The system measurement equation is given by

$$\mathbf{z}_k = \mathbf{h}(\mathbf{x}_k) + \mathbf{w}_k, \tag{3}$$

where the bottom depth measurement $\mathbf{z}$ is either a vector or a scalar, depending on the type of sensor considered. For single measurements, such as single beam echo sounders (SBE), the measurements are scalar, whereas for multibeam echo sounders (MBE) we have vector measurements. The function $\mathbf{h}(\mathbf{x}_k)$ denotes the true sea depth at position $\mathbf{x}_k$, which has to be estimated by a digital terrain map. The vector $\mathbf{w}_k$ denotes the sensor measurement noise, which is assumed to be white.

In order to simplify the mathematical description of our algorithms, we will express our true position as an offset, $\delta\mathbf{x}$, from the position estimate $\tilde{\mathbf{x}}$ of the inertial navigation system. Our process then becomes

$$\delta\mathbf{x}_k = \mathbf{x}_k - \tilde{\mathbf{x}}_k, \tag{4}$$

$$\begin{aligned}\delta\mathbf{x}_{k+1} &= \mathbf{x}_{k+1} - \tilde{\mathbf{x}}_{k+1} \\ &= \mathbf{x}_k + \mathbf{u}_k + \mathbf{v}'_k + \mathbf{v}_k - \tilde{\mathbf{x}}_k - \mathbf{u}_k \\ &= \delta\mathbf{x}_k + \mathbf{v}'_k + \mathbf{v}_k.\end{aligned} \tag{5}$$

B. Filter model

Due to the computational requirements of the point mass filter, we here restrict ourselves to a two-dimensional state vector, representing the horizontal position of the vehicle. As there is no room for additional error states in our state vector, all our noises have to be modeled as white, and we have to consider a simpler system than that in (1)–(3). To distinguish between variables in our system and filter models, we use asterisks for variables in the filter model. Our filter model reads, using the same delta notation as in (4)–(5),

$$\delta\mathbf{x}^*_k = \mathbf{x}^*_k - \tilde{\mathbf{x}}_k, \tag{6}$$

$$\begin{aligned}\delta\mathbf{x}^*_{k+1} &= \mathbf{x}^*_{k+1} - \tilde{\mathbf{x}}_{k+1} = \mathbf{x}^*_k + \mathbf{u}_k + \mathbf{v}^*_k - \tilde{\mathbf{x}}_k - \mathbf{u}_k \\ &= \delta\mathbf{x}^*_k + \mathbf{v}^*_k,\end{aligned} \tag{7}$$

$$\mathbf{z}_k = \mathbf{h}^*(\mathbf{x}^*_k) + \mathbf{w}^*_k = \mathbf{h}^*(\tilde{\mathbf{x}}_k + \delta\mathbf{x}^*_k) + \mathbf{w}^*_k, \tag{8}$$

with the assumptions

$$E\{\mathbf{v}^*_k \mathbf{v}^{*T}_l\} = \mathbf{Q}_k \delta_{kl}, \tag{9}$$

$$E\{\mathbf{w}^*_k \mathbf{w}^{*T}_l\} = \mathbf{R}_k \delta_{kl}, \tag{10}$$

where δ_{kl} denotes the Kronecker delta, such that the noise sequences are uncorrelated from time step to time step. We also need to specify the distributions of the noise sequences and the initial position offset, $\delta\mathbf{x}^*_0$. A convenient, but not necessary, assumption is to assume Gaussian distributions,

$$p(\delta\mathbf{x}^*_0) = \mathcal{N}(\mathbf{0}, \mathbf{P}_0), \tag{11}$$

$$p(\mathbf{v}^*_k) = \mathcal{N}(\mathbf{0}, \mathbf{Q}_k), \tag{12}$$

$$p(\mathbf{w}^*_k) = \mathcal{N}(\mathbf{0}, \mathbf{R}_k). \tag{13}$$

Equation (11) indicates that the initial position has a normal distribution centered around the position $\tilde{\mathbf{x}}_0$, given by the inertial navigation system. We further assume that the process noise, measurement noise and initial position are uncorrelated,

$$E\{\mathbf{v}_k^*\mathbf{w}_l^{*T}\} = \mathbf{0}, \quad (14)$$

$$E\{\mathbf{v}_k^*\mathbf{x}_0^{*T}\} = \mathbf{0}, \quad (15)$$

$$E\{\mathbf{w}_k^*\mathbf{x}_0^{*T}\} = \mathbf{0}, \quad (16)$$

for all k and l. The function $\mathbf{h}^*(\mathbf{x}_k^*)$ indicates the depth at position $\mathbf{x}_k^*$ given by the digital terrain map. We here use terrain maps consisting of gridded nodes, and the depth values given by $\mathbf{h}^*$ are found by bilinear interpolation of the terrain database. The noise sequence $\mathbf{w}_k^*$ in (8) therefore models both map noise (including interpolation errors) and the sensor noise. The measurement $\mathbf{z}_k$ is the total sea depth at the current AUV position, and it is computed as the sum of the AUV depth, given by a pressure sensor, and the AUV altitude above the sea floor, given by the bathymetric sensor. The noise sequence $\mathbf{w}_k^*$ therefore contains contributions from map errors, pressure sensor noise and bathymetric sensor noise. For a detailed analysis of the depth accuracy for the HUGIN class AUVs, we refer to [14].

C. The Recursive Bayesian Filter Equations

Let $\mathbb{Z}_k$ be the augmented measurement vector consisting of all the measurements up to time step k. From Bayes' formula (see e.g. [15]) and our filter model, (6)-(8), we have

$$\begin{aligned} p(\delta\mathbf{x}_k^*|\mathbb{Z}_k) &= \frac{p(\mathbf{z}_k|\delta\mathbf{x}_k^*, \mathbb{Z}_{k-1})p(\delta\mathbf{x}_k^*|\mathbb{Z}_{k-1})}{p(\mathbf{z}_k|\mathbb{Z}_{k-1})} \\ &= \frac{p_{\mathbf{w}_k^*}(\mathbf{z}_k - \mathbf{h}^*(\tilde{\mathbf{x}}_k + \delta\mathbf{x}_k^*))p(\delta\mathbf{x}_k^*|\mathbb{Z}_{k-1})}{\int\limits_{\mathbb{R}^2} p_{\mathbf{w}_k^*}(\mathbf{z}_k - \mathbf{h}^*(\tilde{\mathbf{x}}_k + \delta\mathbf{x}_k^*))p(\delta\mathbf{x}_k^*|\mathbb{Z}_{k-1})\mathrm{d}\delta\mathbf{x}_k^*}. \end{aligned} \quad (17)$$

Our measurement update can then be written as

$$p(\delta\mathbf{x}_k^*|\mathbb{Z}_k) = \alpha^{-1}p_{\mathbf{w}_k^*}(\mathbf{z}_k - \mathbf{h}^*(\tilde{\mathbf{x}}_k + \delta\mathbf{x}_k^*))p(\delta\mathbf{x}_k^*|\mathbb{Z}_{k-1}), \quad (18)$$

where

$$\alpha = \int\limits_{\mathbb{R}^2} p_{\mathbf{w}_k^*}(\mathbf{z}_k - \mathbf{h}^*(\tilde{\mathbf{x}}_k + \delta\mathbf{x}_k^*))p(\delta\mathbf{x}_k^*|\mathbb{Z}_{k-1})\mathrm{d}\delta\mathbf{x}_k^*. \quad (19)$$

The minimum square error (MMSE) estimate is then given by, see [15],

$$\delta\hat{\mathbf{x}}_k = E\{\delta\mathbf{x}_k^*|\mathbb{Z}_k\} = \int\limits_{\mathbb{R}^2} \delta\mathbf{x}_k^* p(\delta\mathbf{x}_k^*|\mathbb{Z}_k)\mathrm{d}\delta\mathbf{x}_k^*, \quad (20)$$

with the estimated covariance matrix

$$\hat{\mathbf{P}}_k = \int\limits_{\mathbb{R}^2} (\delta\mathbf{x}_k^* - \delta\hat{\mathbf{x}}_k^*)(\delta\mathbf{x}_k^* - \delta\hat{\mathbf{x}}_k^*)^T p(\delta\mathbf{x}_k^*|\mathbb{Z}_k)\mathrm{d}\delta\mathbf{x}_k^*. \quad (21)$$

For the time update of our position distribution we have, from conditioning on the position offset from the previous time step and using (7),

$$\begin{aligned} p(\delta\mathbf{x}_{k+1}^*|\mathbb{Z}_k) &= \int\limits_{\mathbb{R}^2} p(\delta\mathbf{x}_{k+1}^*, \delta\mathbf{x}_k^*)\mathrm{d}\delta\mathbf{x}_k^* \\ &= \int\limits_{\mathbb{R}^2} p(\delta\mathbf{x}_{k+1}^*|\mathbb{Z}_k)p(\delta\mathbf{x}_k^*|\mathbb{Z}_k)\mathrm{d}\delta\mathbf{x}_k^* \\ &= \int\limits_{\mathbb{R}^2} p_{\mathbf{v}_k^*}(\delta\mathbf{x}_{k+1}^* - \delta\mathbf{x}_k^*)p(\delta\mathbf{x}_k^*|\mathbb{Z}_k)\mathrm{d}\delta\mathbf{x}_k^*. \end{aligned} \quad (22)$$

Given the distribution of the initial position, $p(\mathbf{x}_0^*)$, the equations (17) and (22) can now be used recursively to obtain the distribution of the position offsets for each time step. The integrals in the equations are, however, not analytically solvable, and we therefore need to evaluate these integrals numerically.

D. Point Mass and Particle Filters

The Point Mass (PMF) and Particle Filters (PF) are numerical estimation methods for solving the optimal Bayesian filter equations (17) and (22). The formulation of the PMF and the Bayesian bootstrap PF algorithms in the framework of terrain aided navigation can be found in [6], wherein it was also concluded that the PMF gives a more robust and stable terrain navigation solution. In the PMF, the probability distribution of the position offset is estimated using a grid of point masses. From the grid approximation, any type of estimate can be computed, including the maximum a posteriori (MAP) estimate and the mean of the posterior, i.e. the MMSE (minimum mean square error) estimate, and its covariance. If the probability density is unimodal, the MAP and MMSE estimates in most cases coincide, whereas in multimodal probability densities the MAP estimate coincides with one of the modes, while the MMSE estimate is located somewhere between the modes. In the results presented herein, the MMSE estimates were used.

III. The HUGIN Real-Time Terrain Navigation System

A. System Overview

The HUGIN Real-Time Terrain Navigation system, named TerrP, is described in detail in [9]. The main purpose of the TerrP system is to provide the main aided inertial navigation system (AINS) with position updates, in a similar manner as any other positioning sensor, like GPS or an acoustic positioning system. The integration is done in a loosely coupled manner. Whenever a new correlation sequence is started, a grid of a certain predefined size and resolution around the current AINS position is defined, and the terrain navigation algorithm is started with a predefined initial probability distribution for the correct position. Variants of the TERCOM and PMF algorithms, see [16]–[18], have been implemented in the TerrP system so far, but due to its modular design, it is straightforward to implement other algorithms in the system. The results presented in this paper are from a 2-dimensional PMF implementation. As new terrain measurements are made

available to the TerrP system, the algorithms are updated recursively, until the proposed terrain navigation (TerrNav) solution satisfies the predefined convergence properties. The converged solution is then subjected to integrity checks, in order to ensure that as few false solutions as possible are sent to the main navigation system. If the solution passes the integrity tests, it is sent to the main AINS, where it is treated as a position measurement in the Kalman filter. Otherwise, the TerrNav solution is not used. In either case, the TerrNav algorithm is restarted, and a new correlation sequence is started. In this way, the main AINS system is provided with a series of TerrNav position updates that are less correlated than what would be the case if the algorithms were never restarted.

B. In situ Sequential Mapping and Localization

In previous terrain navigation tests with the HUGIN vehicles, a prerequisite has been that a terrain map of the area must exist and be uploaded to the vehicle prior to the operation. To extend the application area of the TerrP system, a real-time map generator has been implemented. When TerrP is in mapping mode, the measurements from the bathymetric sensor are used to build up a gridded map database with a predefined resolution. The depth at each node is computed as the running average of all the measurements hitting within the grid cell surrounding the node. Simultaneously, a coarse grid, with typically 2-3 times lower resolution than the main grid, is also built. When the system exits mapping mode, a hole filling procedure is run on the main grid, using interpolation from the coarse grid. The real-time map can later be used for terrain navigation updates, in the exact same manner as when a prior map database is used. When the real-time map is used, the accuracy of the resulting terrain navigation fix is always bounded below by the navigation accuracy at the time of mapping.

IV. Sea Trial Results

A. Description of The Sea Trial

The sea trial was carried out in April 2011, near Larvik in the outer Oslo fjord, as part of a cruise in which a number of new HUGIN technology components were tested. The HUGIN 1000 HUS vehicle, owned by FFI, Kongsberg Maritime and the Institute of Marine Research (IMR), was used for the test, operated from FFI's research vessel H.U. Sverdrup II. For navigation the AUV is equipped with a Honeywell HG9900 inertial measurement unit (IMU), a Teledyne RDI WHN 300 Doppler velocity log (DVL), a Paroscientific Digiquartz pressure sensor and acoustic transponders for HiPAP- (ultra short base line) and UTP (single underwater transponder) navigation. In addition it can carry different sets of payload sensors, such as the EM 2000 multibeam echo sounder and the Kongsberg HISAS 1030 synthetic aperture sonar (SAS). The EM 2000 (200 kHz) was used as terrain navigation sensor in this test, providing up to 111 measurements per ping.

The planned trajectory of the run is shown in Fig. 2, together with sea chart bathymetry of the area. Prior to the test, high resolution bathymetric data from the area was collected from H.U. Sverdrup II, using its Kongsberg EM 710 multibeam echo sounder (MBE). These data were crudely post-processed and used as the basis of a 10 m horizontal resolution gridded DTM (Digital Terrain Model) to be used by the TerrP system during the test. The terrain in the area is highly varying, including some underwater valleys with relatively flat bottom topography within the valleys, and steep valley sides. The total sea depth along the trajectory is seen in Fig. 3. The trajectory was laid out in such a manner that several different terrain types were covered. At the same time, the vehicle was programmed to follow long, relatively straight lines following the same general direction for a long time, in order to avoid error-canceling in the DVL-aided INS, since one of the main purposes of the test was to investigate the ability of the TerrP system to sustain a high navigation accuracy in the overall navigation solution. For a high-quality aided INS (AINS) on an AUV, i.e. without terrain navigation updates, the errors in the heading and velocity measurements integrate to a position error in the order of 0.1–0.2% of traveled distance, mostly depending on the accuracy of the DVL. The total duration of this test was 6 hours and 20 minutes. With an AUV speed of 2 m/s, a navigation drift of 0.1–0.2 % of traveled distance would correspond to about 45–90 m. However, as the mission plan contained some turns, some error canceling should occur, leading to a slower drift. During the test, the surface vessel followed the AUV, providing acoustic measurements that could be used in order to establish a high quality navigation reference solution. This reference solution was calculated using the post-processing tool NavLab, developed by FFI [19]. The estimated horizontal accuracy of this reference solution is within 2 m (1σ). The HiPAP acoustic positioning measurements were not used by the vehicle for real-time navigation.

The purpose of this test was twofold. First, we wanted to further test the system's ability to bind the drift in the navigation system using terrain navigation with MBE as the only position update method. In addition, we wanted to test out the *in situ* sequential mapping and localization mode. The vehicle was therefore programmed to first conduct a lawn-mower pattern in a box of approximately 600 m by 600 m, creating a local real-time map of the area, i.e. TerrP was run in mapping mode. After completing the box area, the vehicle was programmed to conduct a transit phase, following a straight line in a westerly direction. During this phase TerrP was run in normal navigation mode, using the pre-made map. After transiting for about two hours, the vehicle was to return towards the box area. During this phase the TerrP system was set in standby mode, such that no updates were sent to the main navigation system. This was done in order to generate navigation uncertainty, to test whether the system was able to use the previously made real-time map of the box area to obtain a relative position update.

B. Transit Phase

The TerrP system's ability to sustain high navigation accuracy without any other external position measurements has

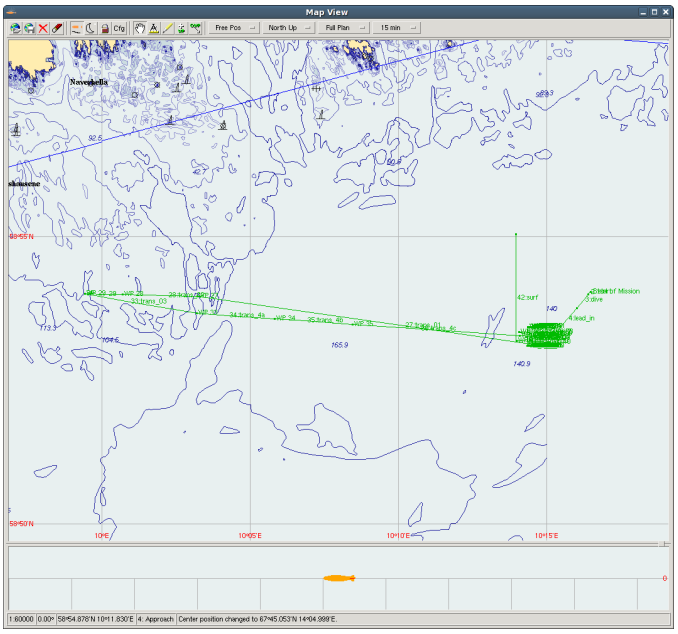

Fig. 2. Overview of the test run, as seen in the HUGIN operator station (HOS) topside.

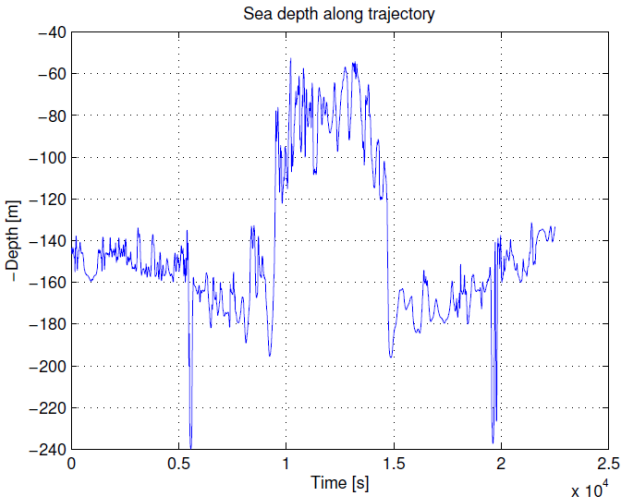

Fig. 3. The total sea depth along the reference trajectory, given by the prior map.

been demonstrated before, e.g. using DVL measurements [8]. The difference between the real time navigation solution, using the converged TerrP fixes as position measurements, and the post-processed reference solution is shown in Fig. 4. After finishing the mapping of the box area, the TerrP system was run in normal navigation mode, using the preloaded map. This corresponds to the period from about 7500 to 18000 seconds in the graph. During this period, the error in the real-time navigation solution is between 5-20 m, which is a little poorer than should be expected when using a map database with 10 m resolution. However, the NavP-NavLab difference is clearly

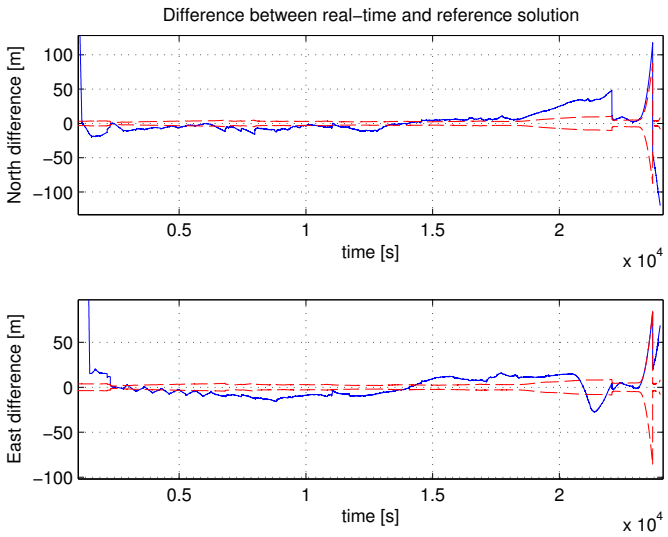

Fig. 4. Difference between real time navigation solution (with TerrP updates) and reference solution. The difference is shown in a solid blue line and the real time estimated standard deviation in red.

outside the estimated 1 σ bounds estimated by NavP, indicating an overconfident real-time navigation solution. When analyzing the navigation data in post-processing, it turned out that there was a fairly constant difference of 5-10 m between the real-time navigation solution and the post-processed position estimates. In Fig 5, which shows the TerrP fixes, the HiPAP measurements and the NavP and NavLab solutions in a portion of the transit phase, this is clearly visible. Notice how most of the TerrP fixes are closer to the NavLab solution and the HiPAP measurements than to the NavP solution. Even a high number of fairly consistent TerrP measurements do not seem to influence the NavP solution enough to bring it closer to the 'true' solution. The fact that both the TerrP fixes and the HiPAP measurements seem to agree well, indicates that the problem is in the NavP solution. During the initialization phase of the INS, HUGIN HUS is kept inside a container on the aft deck of HU Sverdrup II, and receives GPS signals from a GPS repeater. In this sea trial there were problems with the GPS repeater. The initial position used by the INS was over 100 m off, and caused the navigation system to lock on to a wrong heading estimate. The heading estimates from NavP and NavLab from part of the transit phase are shown in Fig. 6. A difference of almost 0.5 degrees is visible, even though the NavP system reports a heading accuracy of 0.02 degrees. This is the reason why the NavP Kalman filter does not weight the TerrP measurements enough to correctly estimate the position error seen in Fig. 5.

C. Box Revisit Phase

As the vehicle approached the box area again, after about 18000 seconds, the TerrP system was set in standby mode, such that main navigation system was run without any position measurements. A contour plot of the real-time map created by the TerrP system in the box area, is shown in Fig. 7. When

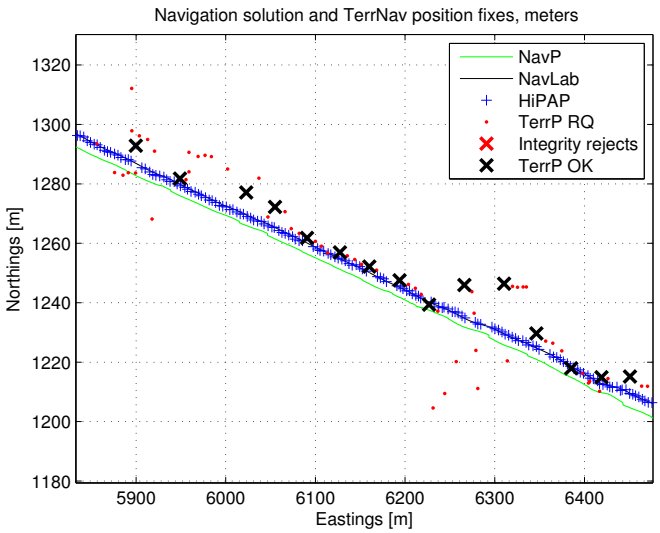

Fig. 5. Terrain navigation position fixes (black crosses = converged fixes, red dots = estimates before convergence), HiPAP measurements, real time navigation and reference solution during transit phase.

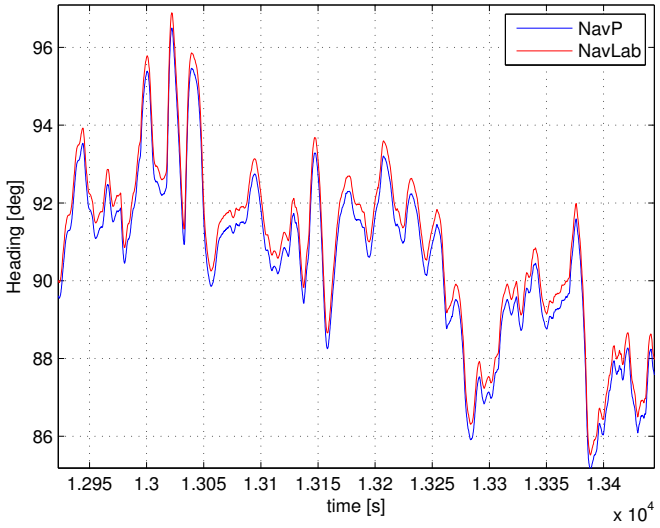

Fig. 6. Heading from real-time (NavP, blue) and post-processed (NavLab, red) navigation solution in a part of the run. A discrepancy of almost 0.5 degrees is visible.

reentering this area, the actual navigation error was more than 50 m, though the estimated uncertainty was underestimated due to the reasons discussed above. As soon as the vehicle was within the area, it was able to compute several good TerrP fixes, which can be seen both in Fig. 8 and Fig. 9, reducing the navigation error to about 10 m. This demonstrates the concept of *in situ* sequential mapping and localization and its ability to obtain relative position fixes using the real-time map.

V. Conclusions

This paper has given a brief overview of the HUGIN AUV terrain navigation system as well as a description of results from a recent sea trial of the system. The sea trial

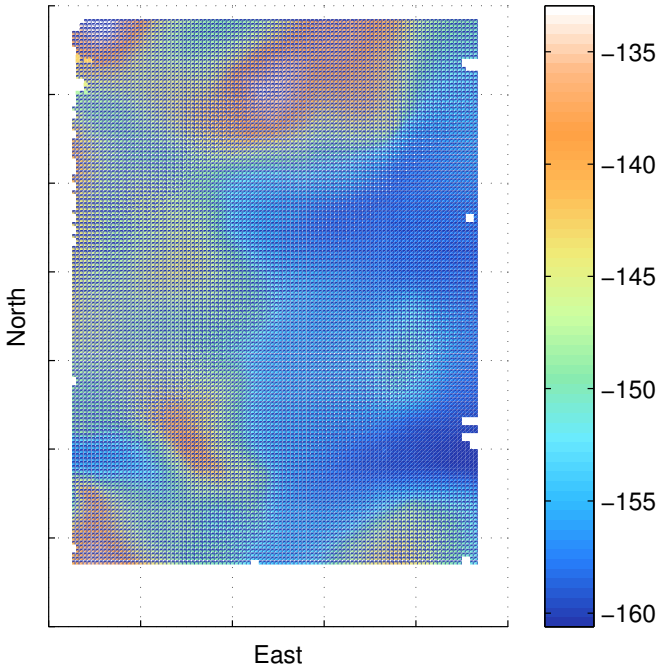

Fig. 7. Real time map created by TerrP mapping engine.

was designed in order to test two different terrain navigation concepts. During the first part of the trial, the vehicle surveyed a small area in a lawn-mower pattern, in order to use a recently developed real-time map generation feature to build up a local map. The map would later be used for obtaining position fixes when returning to the area. This concept is similar to simultaneous localization and mapping (SLAM) and has herein been named '*in situ* sequential mapping and localization'. Using this technique eliminates the need for a prior bathymetric map, which often restricts the operational use of terrain navigation techniques. In the sea trial the actual navigation error, compared to a high quality post-processed navigation solution, was reduced from more than 50 m to about 10 m when reentering the previously mapped area.

The sea trial also contained a transit phase, in which the system's ability to bind the navigation error using multibeam data and a prior bathymetric map database was demonstrated. During this phase, the real-time navigation error stayed within 5–20 m. However, the actual terrain navigation fixes were consistently more accurate than this, when compared to the reference solution. Due to a rare problem with the GPS initialization of the inertial navigation system, the real-time navigation system suffered from overconfidence problems throughout the run and was thus not able to utilize the terrain navigation updates in an optimal manner. On the other hand, the results still demonstrate the ability of the terrain navigation system to sustain a high navigation accuracy without the need of any external position measurements.

The *in situ* sequential mapping and localization technique described in this paper facilitates the use of the terrain nav-

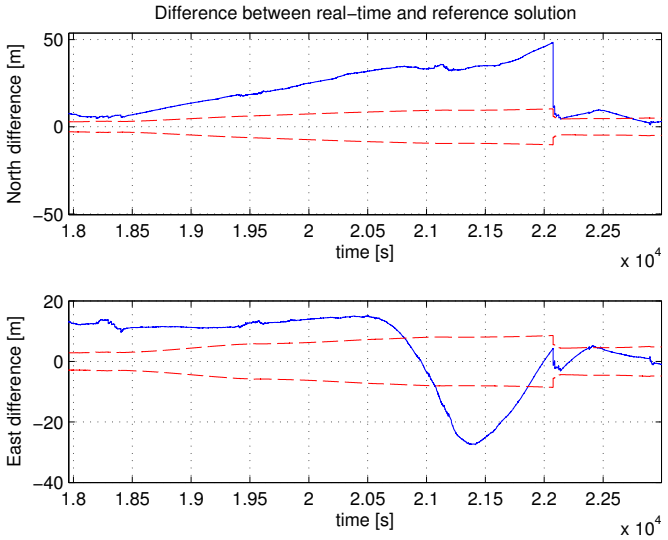

Fig. 8. Difference between real time navigation solution (with TerrP updates) and reference solution when revisiting the box area.

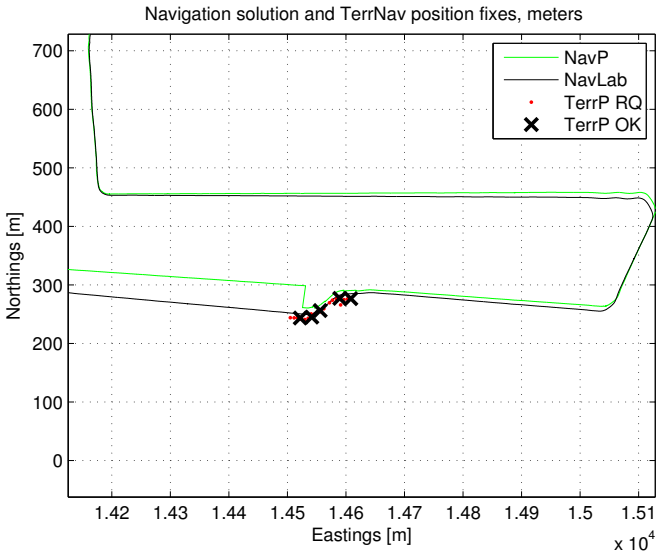

Fig. 9. Terrain navigation position fixes when revisiting the box area.

igation system in a number of new applications without the need of a prior bathymetric map. The theoretical accuracy of this technique is bounded below by the navigation accuracy at the time of mapping. The mapping phase should therefore be carried out as early in the mission as possible. For example, a start line across the operation area could be run in the beginning of the mission, possibly using acoustic position measurements from the surface vessel during the mapping phase. This would result in a highly accurate terrain map along the start line, which could be used for precise terrain navigation updates every time the vehicle crossed the start line later in the mission.

ACKNOWLEDGMENT

The authors wish to thank the crew onboard HU Sverdrup II and the HUGIN operators at FFI for assisting in the collection of the data.

REFERENCES

[1] B. Jalving, K. Gade, O. Hagen, and K. Vestgård, "A toolbox of aiding techniques for the HUGIN AUV integrated inertial navigation system," in *Proceedings of the IEEE Oceans 2003*, San Diego, CA, 2003.

[2] L. Hostetler, "Optimal terrain-aided navigation systems," in *AIAA Guidance an Control Conference*, Palo Alto, CA, 1978.

[3] N. Bergman, "Recursive Bayesian estimation - navigation and tracking applications," Ph.D. dissertation, Department of Electrical Engineering, Linköping University, Sweden, 1999.

[4] I. Nygren and M. Jansson, "Terrain navigation using the correlator method," in *Position Location and Navigation Symposium, PLANS 2004*, Monterey, CA, April 2004.

[5] B. Jalving, M. Mandt, O. Hagen, and F. Pøhner, "Terrain referenced navigation of AUVs and submarines using multibeam echo sounders," in *Proceedings of the UDT Europe 2004*, Nice, France, 2004.

[6] K. Ånonsen and O. Hallingstad, "Terrain aided underwater navigation using point mass and particle filters," in *Proceedings of the IEEE/ION Position Location and Navigation Symposium (PLANS) 2006*, San Diego, CA, April 2006.

[7] K. Ånonsen, O. Hallingstad, and O. Hagen, "Bayesian terrain-based underwater navigation using an improved state-space model," in *Symposium on Underwater Technology and Workshop on Scientific Use of Submarine Cables and Related Technologies, 2007*, Tokyo, Japan, Apr. 2007, pp. 499–505.

[8] K. Ånonsen and O. Hagen, "An analysis of real-time terrain aided navigation results from a HUGIN AUV." in *Proceedings of the IEEE/ION Oceans 2010 Conference*, Seattle, WA, September 2010.

[9] O. Hagen, K. Ånonsen, and M. Mandt, "The HUGIN real-time terrain navigation system," in *Proceedings of the MTS/IEEE Oceans 2010 Conference*, Seattle, WA, USA, September 2010.

[10] J. Carlström, "Results from sea trials of the Swedish AUV62F's terrain navigation system," in *15th International International Symposium on Unmanned Untethered Submersible Technology (UUST'07)*, Durham, NH, USA, 2007.

[11] D. Meduna, S. Rock, and R. McEwen, "Low-cost terrain relative navigation for long-range AUVs." in *MTS/IEEE Oceans 2008 Conference*, Quebec City, QC, Canada, September 2008.

[12] T. Bailey and H. Durrant-Whyte, "Simultaneous localization and mapping (SLAM): Part II State of the art," *IEEE Robotics & Automation Magazine*, vol. 13, no. 3, pp. 108–117, Sep. 2006.

[13] H. Durrant-Whyte and T. Bailey, "Simultaneous localization and mapping (SLAM): Part I The essential algorithms," *IEEE Robotics & Automation Magazine*, vol. 13, no. 2, pp. 99–110, Jun. 2006.

[14] B. Jalving, "Depth accuracy in seabed mapping with underwater vehicles," in *Proceedings of the IEEE Oceans '99*, Seattle, WA, 1999.

[15] Y. Bar-Shalom, X. Li, and T. Kirubarajan, *Estimation with Applications to Tracking and Navigation*. New York: John Wiley & Sons, 2001.

[16] J. Golden, "Terrain contour matching (TERCOM): A cruise missile guidance aid," in *Image Processing for Missile Guidance*, T. Wiener, Ed., vol. 238. San Diego, CA: The Society of Photo-Optical Instrumentation Engineers, 1980, pp. 10–18.

[17] N. Bergman, L. Ljung, and F. Gustafsson, "Terrain navigation using Bayesian statistics," *IEEE Control Systems Magazine*, vol. 19, no. 3, pp. 33–40, Jun. 1999.

[18] K. B. Ånonsen, O. Hallingstad, O. Hagen, and M. Mandt, "Terrain aided AUV navigation - a comparison of the point mass filter and terrain contour matching algorithms," in *Proceedings of the Undersea Defence Technology Conference (UDT) Europe 2005*, Amsterdam, the Netherlands, June 2005.

[19] K. Gade, "NavLab, a generic simulation and post-processing tool for navigation," *European Journal of Navigation*, vol. 2, no. 4, pp. 51–59, November 2004. [Online]. Available: www.navlab.net